CAUCHY – Jurnal Matematika Murni dan Aplikasi
Volume 11 (1) (2026), Pages 473-488
p-ISSN: 2086-0382; e-ISSN: 2477-3344

Stability Analysis and Invasion Thresholds in a Rosenzweig–MacArthur Model with Prey Immigration and Cooperative Hunting

Naufal Daffa Faustin and Dian Savitri*

Department of Mathematics, Universitas Negeri Surabaya, Indonesia

Abstract

Predator–prey systems with multiple interacting ecological mechanisms require integrated modeling approaches for realistic analysis. This study develops a unified Rosenzweig–MacArthur model incorporating both continuous prey immigration and cooperative hunting among predators to analyze how these combined mechanisms affect equilibrium existence, stability, and transient dynamics. Analytical methods derive explicit invasion thresholds and local stability conditions through eigenvalue analysis, while numerical simulations with biologically plausible parameters compare two dynamical regimes: baseline conditions produce stable-node convergence, whereas high-efficiency conditions yield stable-spiral oscillations. Results show that immigration elevates prey density above invasion thresholds, enabling predator persistence, while increased cooperation intensity transitions the system from monotonic to oscillatory convergence. The integrated framework demonstrates how bottom-up (immigration) and top-down (cooperation) processes interact to shape predator–prey dynamics, providing testable predictions for ecosystems where both mechanisms operate simultaneously and establishing a foundation for more complex ecological modeling.

Keywords: cooperative hunting; local stability; predator–prey dynamics; prey immigration; Rosenzweig–MacArthur model

Copyright © 2026 by Authors, Published by CAUCHY Group. This is an open access article under the CC BY-SA License (https://creativecommons.org/licenses/by-sa/4.0)

1. Introduction

Predator–prey interactions constitute a fundamental topic in mathematical biology due to their central role in explaining population regulation, ecological stability, and species coexistence mechanisms [1]. Mathematical models provide an effective framework for representing such interactions by translating biological assumptions into dynamical systems that can be analyzed rigorously [2]. Among the classical formulations, the Lotka–Volterra and Rosenzweig–MacArthur models have been extensively employed to describe oscillatory dynamics and equilibrium behavior in predator–prey systems [3]. However, these classical models often rely on simplifying assumptions that neglect several ecological processes observed in real ecosystems, such as migration, behavioral adaptation, and cooperative interactions [4].

Recent developments in predator–prey modeling have emphasized the importance of incorporating population immigration to improve ecological realism. Immigration, particularly prey

*Corresponding author. E-mail: diansavitri@unesa.ac.id

Submitted: January 24, 2026 Reviewed: February 02, 2026 Accepted: February 20, 2026
DOI: https://doi.org/10.18860/cauchy.v11i1.40677

immigration, has been shown to alter equilibrium configurations and enhance population persistence by preventing extinction scenarios. Analytical studies demonstrate that prey immigration can stabilize otherwise unstable predator–prey systems and expand the parameter regions that allow coexistence [5]. These findings are further supported by comprehensive reviews highlighting immigration as a key mechanism influencing resilience and long-term dynamics in ecological models [6].

In parallel with immigration effects, cooperative hunting among predators has attracted growing attention in recent predator–prey studies [7]. Cooperative predation, where predators coordinate their hunting strategies, can significantly increase capture efficiency and modify the functional response structure [8]. Mathematical investigations reveal that cooperative hunting may fundamentally change equilibrium structures, local stability properties, and bifurcation behavior in predator–prey systems [9]. Such models often exhibit richer dynamical patterns compared to non-cooperative formulations [10].

Despite substantial progress, most existing studies consider prey immigration and cooperative hunting as separate mechanisms [11]. Only a limited number of models attempt to integrate multiple ecological processes simultaneously, even though real ecosystems are influenced by interacting mechanisms operating concurrently [12]. The lack of models that jointly incorporate prey immigration and cooperative hunting represents a notable gap in the current literature, particularly within the Rosenzweig–MacArthur modeling framework [13].

From a mathematical standpoint, the investigation of equilibrium points and their local stability remains a core objective in predator–prey modeling [14]. Local stability analysis provides insight into the response of ecological systems to small perturbations around equilibrium states. Analytical tools such as Jacobian matrices and eigenvalue analysis offer rigorous criteria for stability classification, while numerical simulations are widely used to illustrate transient dynamics and validate analytical predictions [15].

Motivated by these considerations, the present study aims to develop and analyze an extended Rosenzweig–MacArthur predator–prey model that incorporates continuous prey immigration and cooperative hunting among predators [16]. The Rosenzweig–MacArthur structure is chosen because it explicitly incorporates a saturating functional response (Holling type II), which is essential for capturing the saturation effects of predation, especially when cooperation modifies encounter rates. The cooperative functional response $\frac{\beta(1+\alpha y)x}{m+(1+\alpha y)x}$ extends the classical form by letting the cooperation factor $(1 + \alpha y)$ scale both the numerator (effective attack rate) and denominator (handling saturation), thereby maintaining analytical tractability while incorporating cooperation in a biologically interpretable way.

The novelty of this work is threefold. First, we derive an explicit predator-invasion threshold $H = dm/(\mu - d)$ and show how prey immigration elevates the prey density above this threshold, enabling predator persistence. Second, we obtain analytical trace–determinant expressions that govern the local stability of the coexistence equilibrium. Third, we identify the parameter-driven transition from stable node (real eigenvalues) to stable spiral (complex eigenvalues) as cooperation intensity α increases. These mathematical contributions address the following research questions: (i) Under what conditions does a feasible coexistence equilibrium exist? (ii) How do immigration and cooperation affect the local stability of equilibria? (iii) Does the system exhibit oscillatory dynamics, and what parameter shifts lead to such behavior?

The main contribution of this study lies in integrating prey immigration and cooperative predation within a single analytical framework, thereby providing a more realistic representation of predator–prey dynamics compared to existing models that treat these mechanisms separately [13].

The remainder of this paper is organized as follows. Section 2 presents the model formulation and analytical methods, Section 3 discusses the analytical and numerical results, and Section 4 concludes the paper with final remarks and future research directions.

2. Methods

This study examines predator–prey dynamics with prey immigration and cooperative hunting using a combined analytical–numerical framework. A unified mathematical model is constructed by incorporating a cooperative hunting mechanism into a Rosenzweig–MacArthur predator–prey structure with continuous prey immigration [6]. The Rosenzweig–MacArthur formulation is adopted due to its explicit saturating functional response, which allows cooperative effects on predation to be modeled consistently while retaining analytical tractability. The qualitative dynamical properties of the resulting system including equilibrium existence, predator invasion conditions, and local stability are analyzed using standard tools from nonlinear dynamical systems theory [17], while numerical simulations are employed to illustrate local dynamical behavior under biologically plausible parameter regimes.

2.1. Cooperative hunting in a predator-prey model

Cooperative hunting among predators enhances predation efficiency through coordinated foraging, leading to predator-dependent predation rates where capture success increases with predator density [8]. A representative mathematical formulation was proposed by Berec [6], in which cooperative effects are incorporated explicitly into the functional response.

Parameter clarification: In the unified model, $\alpha \geq 0$ quantifies the *intensity of cooperative hunting*, scaling how predator density enhances predation efficiency. In contrast, β represents the *maximum per-capita attack rate* under standard (non-cooperative) conditions. This distinction is maintained throughout the analysis to avoid conceptual ambiguity.

The predator–prey model considered by Berec is given by

$$\begin{aligned} \frac{dx}{dt} &= x\left(\frac{b}{1+\beta y} - d - x - \frac{(1+\alpha y)\,y}{p+(1+\alpha y)x}\right), \\ \frac{dy}{dt} &= y\left(1 - \frac{qy}{r+(1+\alpha y)x}\right), \end{aligned} \tag{1}$$

where $x(t)$ and $y(t)$ denote prey and predator densities at time t, respectively [6]. Here b is the intrinsic growth rate of the prey population, while β quantifies a fear effect induced by predator presence on prey growth [18]. The parameter d denotes the natural death rate of prey, and p and r are positive constants associated with saturation effects in the predation process. The parameter $\alpha \geq 0$ measures the intensity of cooperative hunting among predators.

The cooperative effect enters the model through the multiplicative factor $(1 + \alpha y)$ appearing in both the numerator and denominator of the functional response. This structure reflects that cooperation increases the effective encounter rate between predators and prey (numerator), while simultaneously influencing handling-time saturation (denominator), providing a mathematically consistent predator-dependent Holling type II functional response [6]. When $\alpha = 0$, the model reduces to a Leslie–Gower type predator–prey system without cooperative interactions [19]. Berec demonstrated that this cooperative structure can substantially modify equilibrium existence and local stability properties compared to traditional non-cooperative models [20].

2.2. Rosenzweig–MacArthur model with prey immigration

In the Rosenzweig–MacArthur framework, prey immigration is commonly introduced as a constant external input $c \geq 0$, representing continuous influx from neighboring habitats without requiring explicit spatial terms [5]. This formulation preserves analytical tractability while capturing the stabilizing effect of immigration on predator–prey coexistence [21]. Moreover, the Rosenzweig–MacArthur model incorporates a saturating (Holling type II) functional response, which is particularly suitable for extensions involving predator behavioral mechanisms.

A standard Rosenzweig–MacArthur model with Holling type II functional response and constant prey immigration, analyzed by Sugie and Saito [6], is given by

$$\begin{aligned} \frac{dx}{dt} &= rx\left(1-\frac{x}{K}\right) - \frac{xy}{a+x} + c, \\ \frac{dy}{dt} &= y\left(\frac{\mu x}{a+x} - d\right), \end{aligned} \tag{2}$$

where $x(t)$ and $y(t)$ are prey and predator densities, r and K are the prey intrinsic growth rate and carrying capacity, a is the half-saturation constant, μ is the conversion efficiency, and d is the predator mortality rate. The immigration term c directly augments the prey equation, ensuring a minimum prey supply even under high predation pressure.

Sugie and Saito showed that immigration can prevent extinction, expand coexistence regions, and alter oscillatory dynamics [6]. In the present study, this immigration structure is retained as a baseline component, while the functional response is systematically modified to incorporate cooperative hunting effects within the Rosenzweig–MacArthur framework.

2.3. Analytical methods

The analytical component follows standard techniques from nonlinear dynamical systems theory applied to predator–prey models. Equilibrium points are obtained by solving the steady-state conditions $\frac{dx}{dt} = 0$ and $\frac{dy}{dt} = 0$. Local stability of each equilibrium is determined via linearization: the Jacobian matrix is computed symbolically, and its eigenvalues are analyzed using the characteristic equation $\det(J - \lambda I) = 0$. For two-dimensional systems, stability is classified using the Routh–Hurwitz criteria, requiring a negative trace and a positive determinant of the Jacobian [22]. Transitions between stable nodes and stable spirals are identified through the discriminant condition $\mathrm{tr}^2(J) - 4\det(J)$.

To characterize predator persistence, invasion conditions are derived by evaluating the predator growth rate in a neighborhood of the prey-only equilibrium. These methods are well established for Rosenzweig–MacArthur type models with additional ecological mechanisms such as immigration and cooperative behavior [5]. All symbolic derivations are carried out manually and verified for algebraic consistency, and explicit expressions for equilibria and Jacobian entries are provided in the Results section.

2.4. Numerical methods

To complement the analytical results, numerical simulations are carried out to illustrate the qualitative dynamics predicted by the local stability analysis under different parameter regimes using *Maple*. Time-series solutions and phase portraits are generated to visualize transient behavior, oscillatory responses, and convergence toward equilibrium states. The numerical procedures follow established practices in ecological modeling studies involving prey immigration and cooperative hunting [6].

Numerical simulations serve as illustrative tools, not as a basis for global-stability claims. Two contrasting scenarios are examined: a baseline regime with moderate predation and weak cooperation, and a high-efficiency regime with elevated attack rate and strong cooperation. These scenarios bracket plausible ecological conditions and demonstrate the model's capacity to generate both nodal and spiral convergence under ecologically documented parameter ranges.

3. Results and Discussion

This section presents the analytical and numerical results for the predator–prey model that incorporates both prey immigration and cooperative hunting. The presentation follows the research questions outlined in the Introduction: first, the unified model is constructed; second, its equilibria and local stability are analyzed; third, numerical simulations illustrate the parameter-dependent dynamics.

3.1. Model construction

The proposed model integrates the cooperative hunting mechanism of Berec with the immigration-extended Rosenzweig–MacArthur framework of Sugie and Saito [1]. The cooperative Holling type II functional response

$$\frac{\beta(1+\alpha y)x}{m+(1+\alpha y)x}$$

is adopted directly from Berec. The factor $(1+\alpha y)$ multiplies both the numerator and denominator because cooperation increases the effective encounter rate between predators and prey (numerator) while simultaneously affecting handling-time saturation (denominator). This preserves the saturating form of the Holling type II response while making the half-saturation density $m/(1+\alpha y)$ decrease with predator density, which is a hallmark of cooperative hunting.

The resulting system is given by

$$\begin{aligned} \frac{dx}{dt} &= rx\left(1-\frac{x}{K}\right) - \frac{\beta(1+\alpha y)xy}{m+(1+\alpha y)x} + c, \\ \frac{dy}{dt} &= \frac{\mu(1+\alpha y)xy}{m+(1+\alpha y)x} - dy, \end{aligned} \tag{3}$$

where $x(t)$ and $y(t)$ denote prey and predator densities, respectively. The parameters r and K represent the intrinsic growth rate and carrying capacity of the prey, m is the half-saturation constant, β is the maximum attack rate, $\alpha \geq 0$ quantifies the intensity of cooperative hunting, μ is the conversion efficiency, d is the predator mortality rate, and $c \geq 0$ denotes the constant prey immigration rate.

The model reduces to the classical Rosenzweig–MacArthur system with immigration when $\alpha = 0$, to a cooperative hunting model without immigration when $c = 0$, and to the standard Rosenzweig–MacArthur model when $\alpha = c = 0$. Hence, system Eq. (3) provides a unified framework for studying the combined effects of prey immigration and predator cooperation. The variables and parameters of the model are summarized in Table 1.

Table 1: Variables and parameters of the proposed predator–prey model

Symbol	Type	Description	Unit
$x(t)$	Variable	Prey population density	Population
$y(t)$	Variable	Predator population density	Population
r	Parameter	Intrinsic growth rate of the prey	Time^{-1}
K	Parameter	Environmental carrying capacity of the prey	Population
m	Parameter	Half-saturation constant of the functional response	Population
β	Parameter	Maximum attack rate of predators	Time^{-1}
α	Parameter	Intensity of cooperative hunting among predators	Dimensionless
μ	Parameter	Conversion efficiency of prey into predator biomass	Dimensionless
d	Parameter	Natural mortality rate of predators	Time^{-1}
c	Parameter	Constant prey immigration rate	Population·Time^{-1}

3.2. Model analysis

We investigate the qualitative behavior of system Eq. (3) by determining its equilibrium points and analyzing their local stability. Equilibrium points represent population states where both prey and predator densities remain constant over time, obtained by solving

$$\frac{dx}{dt} = 0, \qquad \frac{dy}{dt} = 0. \tag{4}$$

3.2.1. Predator-free equilibrium

Theorem 3.1. *For system Eq. (3) with parameters $r > 0$, $K > 0$, $c \geq 0$, there exists a unique biologically feasible predator-free equilibrium $E_1 = (x_1, 0)$, where*

$$x_1 = \frac{K}{2}\Big(1 + \sqrt{1 + \frac{4c}{rK}}\Big) > 0. \tag{5}$$

Proof. When predators are absent ($y = 0$), the predator equation $\frac{dy}{dt} = 0$ is automatically satisfied. Substituting $y = 0$ into the prey equation gives

$$rx\Big(1 - \frac{x}{K}\Big) + c = 0. \tag{6}$$

This quadratic equation rearranges to

$$x^2 - Kx - \frac{Kc}{r} = 0, \tag{7}$$

with discriminant $\Delta = K^2 + \frac{4Kc}{r} > 0$. The quadratic formula yields two solutions:

$$x_{1,2} = \frac{K \pm \sqrt{K^2 + \frac{4Kc}{r}}}{2}. \tag{8}$$

Only the positive root is biologically meaningful, giving

$$x_1 = \frac{K}{2}\Big(1 + \sqrt{1 + \frac{4c}{rK}}\Big) > 0. \tag{9}$$

Thus $E_1 = (x_1, 0)$. When $c = 0$, we recover $x_1 = K$, the usual carrying capacity without immigration. □

3.2.2. Interpretation of predator-free equilibrium

The predator-free equilibrium E_1 depends critically on the immigration rate c. For $c = 0$, $x_1 = K$ corresponds to the classical logistic carrying capacity. For $c > 0$, immigration raises the prey density above the environmental carrying capacity: $x_1 > K$. This excess prey availability creates conditions favorable for predator invasion when

$$\frac{\mu x_1}{m + x_1} > d \quad \Longleftrightarrow \quad x_1 > \frac{dm}{\mu - d} =: H. \tag{10}$$

The case $c < 0$ (emigration or harvesting) is biologically irrelevant here.

3.2.3. Coexistence equilibrium

Theorem 3.2 (Existence and uniqueness of the coexistence equilibrium)**.** *Assume $\mu > d$ and define*

$$H := \frac{dm}{\mu - d} > 0. \tag{11}$$

Coexistence equilibria $E_2 = (x^*, y^*)$ with $x^*, y^* > 0$ correspond exactly to positive roots $y^* > 0$ of the scalar equation

$$F(y) = rH\left(1 - \frac{H}{K(1 + \alpha y)}\right) - \frac{\beta H y(1 + \alpha y)}{m + H} + c(1 + \alpha y) = 0. \tag{12}$$

The following sufficient conditions hold:

Existence. *If*

$$rH\left(1-\frac{H}{K}\right)+c>0, \tag{13}$$

then at least one positive coexistence equilibrium exists.

Uniqueness. *If, in addition,*

$$\frac{rH^2\alpha}{K}-\frac{\beta H}{m+H}+c\alpha<0, \tag{14}$$

then the coexistence equilibrium is unique. This condition provides a sufficient (not necessary) criterion ensuring strict monotonicity of F.

Proof. The proof proceeds in five logical steps.

Step 1: Reduction via the predator equation. For an interior equilibrium we require $\frac{dx}{dt}=0$ and $\frac{dy}{dt}=0$. From $\frac{dy}{dt}=0$ with $y>0$,

$$\frac{\mu(1+\alpha y)x}{m+(1+\alpha y)x}-d=0 \quad\Longleftrightarrow\quad (\mu-d)(1+\alpha y)x=dm. \tag{15}$$

Since $\mu>d$ is necessary for predator persistence, define

$$H:=\frac{dm}{\mu-d}>0, \tag{16}$$

which yields

$$(1+\alpha y)x=H \quad\Longleftrightarrow\quad x=\frac{H}{1+\alpha y}. \tag{17}$$

Step 2: Reduction to a scalar equation. Substituting Eq. (17) into $\frac{dx}{dt}=0$ and noting that $m+(1+\alpha y)x=m+H$, we obtain

$$r\frac{H}{1+\alpha y}\left(1-\frac{H}{K(1+\alpha y)}\right)-\frac{\beta Hy}{m+H}+c=0. \tag{18}$$

Multiplying by $(1+\alpha y)$ yields $F(y)=0$ with F defined in Eq. (12). Thus coexistence equilibria correspond exactly to positive roots of F.

Step 3: Existence via the Intermediate Value Theorem. Evaluating at $y=0$ gives

$$F(0)=rH\left(1-\frac{H}{K}\right)+c. \tag{19}$$

If this quantity is positive, then $F(0)>0$. As $y\to\infty$, the dominant term of $F(y)$ is

$$-\frac{\beta H\alpha}{m+H}\,y^2, \tag{20}$$

so $\lim_{y\to\infty}F(y)=-\infty$. Since F is continuous on $[0,\infty)$ and changes sign, the Intermediate Value Theorem guarantees at least one positive root $y^*>0$.

Step 4: Uniqueness via monotonicity. Differentiating F yields

$$F'(y) = \frac{rH^2\alpha}{K(1+\alpha y)^2} - \frac{\beta H}{m+H}(1+2\alpha y) + c\alpha. \tag{21}$$

For all $y \geq 0$,

$$\frac{rH^2\alpha}{K(1+\alpha y)^2} \leq \frac{rH^2\alpha}{K}. \tag{22}$$

Hence,

$$F'(y) \leq \frac{rH^2\alpha}{K} - \frac{\beta H}{m+H} + c\alpha. \tag{23}$$

If this upper bound is negative, then $F'(y) < 0$ for all $y \geq 0$, so F is strictly decreasing on $[0, \infty)$. A strictly decreasing continuous function with $F(0) > 0$ and $\lim_{y\to\infty} F(y) = -\infty$ possesses exactly one positive root. Therefore, under the stated sufficient condition, the coexistence equilibrium is unique.

Step 5: Construction of the equilibrium. For the unique y^* satisfying $F(y^*) = 0$, define

$$x^* = \frac{H}{1+\alpha y^*}. \tag{24}$$

Then (x^*, y^*) satisfies both steady-state equations, completing the proof. □

3.2.4. Jacobian matrix for linearization

Write the right-hand sides of Eq. (3) as

$$f(x,y) = rx\Big(1 - \frac{x}{K}\Big) - \frac{\beta(1+\alpha y)xy}{m+(1+\alpha y)x} + c, \tag{25}$$

$$g(x,y) = y\Big(\frac{\mu(1+\alpha y)x}{m+(1+\alpha y)x} - d\Big). \tag{26}$$

The Jacobian matrix is

$$J(x,y) = \begin{pmatrix} \dfrac{\partial f}{\partial x} & \dfrac{\partial f}{\partial y} \\ \dfrac{\partial g}{\partial x} & \dfrac{\partial g}{\partial y} \end{pmatrix}. \tag{27}$$

with partial derivatives

$$\frac{\partial f}{\partial x} = r\Big(1 - \frac{2x}{K}\Big) - \frac{\beta(1+\alpha y)y}{m+(1+\alpha y)x} + \frac{\beta(1+\alpha y)^2xy}{[m+(1+\alpha y)x]^2}, \tag{28}$$

$$\frac{\partial f}{\partial y} = -\frac{\beta\alpha xy}{m+(1+\alpha y)x} - \frac{\beta(1+\alpha y)x}{m+(1+\alpha y)x} + \frac{\beta\alpha(1+\alpha y)x^2y}{[m+(1+\alpha y)x]^2}, \tag{29}$$

$$\frac{\partial g}{\partial x} = y\Big[\frac{\mu(1+\alpha y)}{m+(1+\alpha y)x} - \frac{\mu(1+\alpha y)^2x}{[m+(1+\alpha y)x]^2}\Big], \tag{30}$$

$$\frac{\partial g}{\partial y} = \frac{\mu(1+\alpha y)x}{m+(1+\alpha y)x} - d + y\Big[\frac{\mu\alpha x}{m+(1+\alpha y)x} - \frac{\mu\alpha(1+\alpha y)x^2}{[m+(1+\alpha y)x]^2}\Big]. \tag{31}$$

3.2.5. Stability of the predator-free equilibrium E_1

Evaluating J at $E_1 = (x_1, 0)$ gives

$$J(E_1) = \begin{pmatrix} r\Big(1 - \dfrac{2x_1}{K}\Big) - \dfrac{c}{x_1} & -\dfrac{\beta x_1}{m + x_1} \\ 0 & \dfrac{\mu x_1}{m + x_1} - d \end{pmatrix}. \tag{32}$$

The eigenvalues are the diagonal entries:

$$\lambda_1^{(1)} = r\Big(1 - \frac{2x_1}{K}\Big) - \frac{c}{x_1}, \qquad \lambda_2^{(1)} = \frac{\mu x_1}{m + x_1} - d. \tag{33}$$

E_1 is locally asymptotically stable if both eigenvalues have negative real parts. The sign of $\lambda_2^{(1)}$ determines predator invasion: $\lambda_2^{(1)} > 0$ (equivalently $x_1 > H$) allows predators to invade the predator-free state.

3.2.6. Stability of the coexistence equilibrium E_2

At $E_2 = (x^*, y^*)$ define $Q = 1 + \alpha y^*$ and recall $x^* = H/Q$. Substituting into Eqs. (28)– (31) and simplifying yields

$$J(E_2) = \begin{pmatrix} a_{11} & a_{12} \\ a_{21} & a_{22} \end{pmatrix}, \tag{34}$$

where

$$a_{11} = r\Big(1 - \frac{2H}{KQ}\Big) - \frac{\beta Q y^*}{m + H} + \frac{\beta H y^*}{(m + H)^2}, \tag{35}$$

$$a_{12} = -\frac{\beta H}{m + H}\Big(1 + \alpha y^* - \frac{\alpha H y^*}{m + H}\Big), \tag{36}$$

$$a_{21} = \frac{\mu Q y^*}{m + H}\Big(1 - \frac{H}{m + H}\Big), \tag{37}$$

$$a_{22} = \frac{\mu \alpha H y^*}{m + H}\Big(1 - \frac{H}{m + H}\Big). \tag{38}$$

The characteristic equation is $\lambda^2 - T\lambda + D = 0$, where

$$T = \operatorname{tr} J(E_2) = a_{11} + a_{22}, \tag{39}$$

$$D = \det J(E_2) = a_{11}a_{22} - a_{12}a_{21}. \tag{40}$$

Explicitly,

$$T = r\Big(1 - \frac{2H}{KQ}\Big) - \frac{\beta Q y^*}{m + H} + \frac{\beta H y^*}{(m + H)^2} + \frac{\mu \alpha H y^*}{m + H}\Big(1 - \frac{H}{m + H}\Big), \tag{41}$$

$$D = \Big[r\Big(1 - \frac{2H}{KQ}\Big) - \frac{\beta Q y^*}{m + H} + \frac{\beta H y^*}{(m + H)^2}\Big] \cdot \frac{\mu \alpha H y^*}{m + H}\Big(1 - \frac{H}{m + H}\Big) \tag{42}$$

$$+ \frac{\beta H}{m + H}\Big(1 + \alpha y^* - \frac{\alpha H y^*}{m + H}\Big) \cdot \frac{\mu Q y^*}{m + H}\Big(1 - \frac{H}{m + H}\Big). \tag{43}$$

For a 2×2 system, the Routh–Hurwitz stability criteria require $T < 0$ and $D > 0$. When both hold, E_2 is locally asymptotically stable. The discriminant $\Delta_s = T^2 - 4D$ determines the type of stable equilibrium: $\Delta_s > 0$ gives a stable node (real eigenvalues), $\Delta_s < 0$ gives a stable spiral (complex eigenvalues with negative real part).

3.2.7. Interpretation of parameter effects

- **Immigration** ($c > 0$): Raises x_1, making $\lambda_2^{(1)}$ more likely positive, destabilizing E_1 and enlarging the parameter region where coexistence is possible.
- **Cooperation intensity** ($\alpha > 0$): Enhances effective attack rate via $(1 + \alpha y)$. In $J(E_2)$, α appears in a_{12}, a_{21}, and a_{22}, strengthening prey–predator coupling. Larger α tends to make T less negative and can eventually cause T to change sign, indicating loss of stability and possible transition to a stable spiral.
- **Attack rate** (β): Directly scales predation pressure; higher β typically reduces x^* and influences T and D.
- **Conversion efficiency** (μ): Affects $H = dm/(\mu - d)$; larger μ (relative to d) increases H, raising both x^* and y^* at coexistence.

3.3. Numerical simulations

To complement the analytical results obtained in the previous section, numerical simulations of system Eq. (3) are carried out using *Maple*. The simulations are designed to (i) numerically evaluate the equilibrium points derived analytically for a given parameter set, (ii) verify their local stability through eigenvalue analysis of the Jacobian matrix, and (iii) illustrate the qualitative dynamical behavior of the system via phase portraits and time-series plots.

The parameter values used in the simulations are:

$$r = 0.28, \quad K = 10, \quad \alpha = 0.05, \quad \beta = 0.1, \quad m = 4, \quad \mu = 0.04, \quad d = 0.02, \quad c = 1.$$

These values are selected to represent a biologically plausible predator–prey system with prey immigration and cooperative hunting, while satisfying the fundamental model assumptions. In particular, the condition $\mu > d$ ensures the feasibility of predator persistence. All parameters are positive, as required in Table 1, and the numerical simulations are intended to illustrate typical system behavior rather than to fit empirical data.

3.3.1. Equilibrium points and feasibility

For the parameter values specified in the numerical simulations, system Eq. (3) admits five equilibrium solutions obtained by solving the associated nonlinear algebraic equations numerically:

$$\begin{aligned}
\tilde{E}_1 &= (12.7919,\, 0),\\
\tilde{E}_2 &= (-2.7919,\, 0),\\
\tilde{E}_3 &= (1.6735,\, 27.8033),\\
\tilde{E}_4 &= (14.2971,\, -14.4045),\\
\tilde{E}_5 &= (-5.9706,\, -33.3989).
\end{aligned}$$

The equilibria $\tilde{E}_1$ and $\tilde{E}_2$ correspond to predator-free steady states arising from the prey equation with immigration, whereas $\tilde{E}_3$, $\tilde{E}_4$, and $\tilde{E}_5$ are obtained from the coexistence conditions involving both species.

From a biological perspective, only equilibria located in the first quadrant ($x \geq 0$, $y \geq 0$) are admissible. Consequently, $\tilde{E}_2$, $\tilde{E}_4$, and $\tilde{E}_5$ are excluded due to negative prey and/or predator densities. The system dynamics under the chosen parameter set are therefore governed by two biologically relevant equilibria:

$$E_1 = \tilde{E}_1 = (12.7919, 0) \quad \text{(predator-free)}, \qquad E_2 = \tilde{E}_3 = (1.6735, 27.8033) \quad \text{(coexistence)}.$$

Here E_1 and E_2 follow the notation established in the analytical section, while the tilde notation distinguishes the raw numerical outputs.

3.3.2. Local stability classification

For the baseline parameter values $r = 0.28$, $K = 10$, $\beta = 0.1$, $\alpha = 0.05$, $m = 4$, $\mu = 0.04$, $d = 0.02$, $c = 1$, the Jacobian matrix of system Eq. (3) is evaluated at each equilibrium point, and the corresponding eigenvalues are computed numerically.

(a) **Predator-free equilibrium** $E_1 = (12.7919, 0)$: The eigenvalues are

$$\lambda_1 = -0.4363, \qquad \lambda_2 = 0.0105.$$

Since $\lambda_2 > 0$, E_1 is a **saddle point**. This confirms the analytical invasion condition from Theorem 3.1: substituting $x_1 = 12.7919$ gives $\mu x_1/(m + x_1) \approx 0.0305 > d = 0.02$. Consequently, the prey density satisfies $x_1 > H$, where $H = dm/(\mu - d) \approx 4$, allowing predator invasion.

(b) **Coexistence equilibrium** $E_2 = (1.6735, 27.8033)$: The characteristic polynomial of the Jacobian at E_2 is $\lambda^2 + T\lambda + D = 0$ with trace $T = -0.2232 < 0$ and determinant $D = 0.00939 > 0$. Because $T^2 - 4D \approx 0.0123 > 0$, both eigenvalues are real and negative:

$$\lambda_1 = -0.1670, \qquad \lambda_2 = -0.0562.$$

Hence E_2 is a **stable node**. The conditions $T < 0$ and $D > 0$ ensure local asymptotic stability, while $T^2 > 4D$ confirms the absence of complex eigenvalues. In the linearized system, convergence toward E_2 is therefore exponential and non-oscillatory. This classification is local and does not preclude nonlinear transient dynamics away from the equilibrium.

3.3.3. Phase portraits for contrasting parameter regimes

Phase portraits illustrating two distinct dynamical regimes of system Eq. (3) are presented in Figures Fig. 1 and Fig. 2.

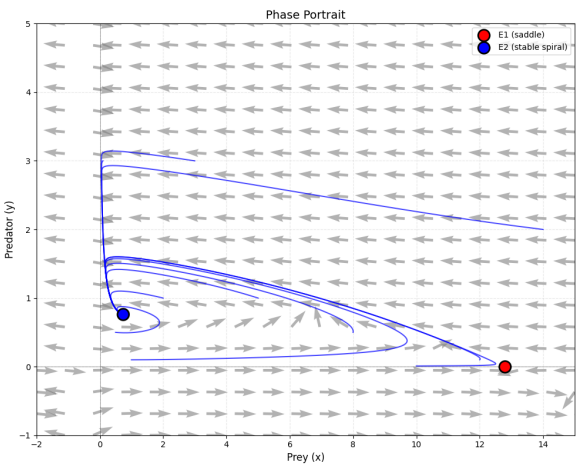

Fig. 1: Phase portrait under high predation efficiency and strong cooperative hunting. Parameters: $\beta = 3.1$, $\alpha = 0.5$, $m = 1$, $\mu = 0.4$, $d = 0.2$, with $r = 0.28$, $K = 10$, $c = 1$.

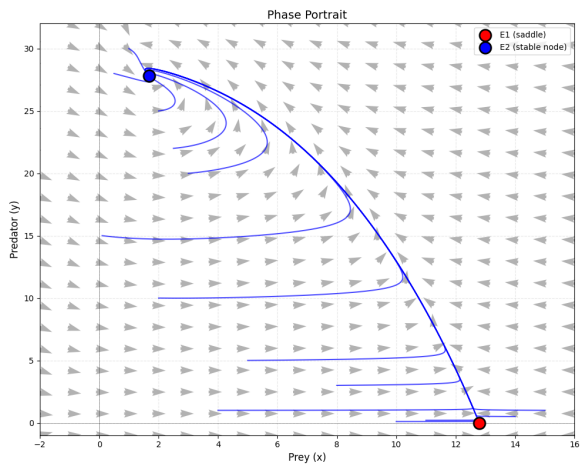

Fig. 2: Phase portrait under baseline parameter values: $\beta = 0.1$, $\alpha = 0.05$, $m = 4$, $\mu = 0.04$, $d = 0.02$, with $r = 0.28$, $K = 10$, $c = 1$.

Both figures display the prey population x on the horizontal axis and the predator population y on the vertical axis, together with the associated direction fields and representative trajectories. In Fig. 1, the parameter set corresponds to high predation efficiency combined with strong cooperative hunting, reduced handling time, and modified predator demographic parameters. Under these conditions, the coexistence equilibrium $E_2 = (0.7230, 0.7663)$ is a **stable spiral**, as indicated by the complex conjugate eigenvalues $\lambda = -0.2771 \pm 0.3068i$. The negative real part ensures local asymptotic stability, while the nonzero imaginary part produces damped oscillations.

The predator-free equilibrium $E_1 = (12.7919, 0)$ remains a saddle point, consistent with the analytical invasion threshold condition.

In contrast, Fig. 2 illustrates the dynamics under the baseline parameter values used throughout the numerical simulations ($\beta = 0.1$, $\alpha = 0.05$, $m = 4$, $\mu = 0.04$, $d = 0.02$, $r = 0.28$, $K = 10$, $c = 1$). Here, the coexistence equilibrium $E_2 = (1.6735, 27.8033)$ is a **stable node**, characterized by real negative eigenvalues $\lambda_1 = -0.1670$ and $\lambda_2 = -0.0562$. Consequently, trajectories converge monotonically toward equilibrium without oscillatory behavior. As in the previous regime, the predator-free equilibrium E_1 exhibits saddle-type instability.

A comparison of the two regimes reveals pronounced differences in both equilibrium densities and convergence behavior. The high-efficiency regime in Fig. 1 combines elevated attack rate ($\beta = 3.1$), strong cooperative hunting ($\alpha = 0.5$), reduced handling time ($m = 1$), and modified predator demographic parameters ($\mu = 0.4$, $d = 0.2$), leading to lower predator density and oscillatory convergence. In contrast, the baseline regime in Fig. 2 employs moderate parameter values and yields higher predator density with direct, non-oscillatory convergence.

These contrasting stability types are consistent with the eigenvalue structure of the Jacobian matrix evaluated at E_2 and highlight the sensitivity of local dynamics to variations in predation efficiency, cooperative effects, and handling time. The observed differences therefore arise from a combination of ecological factors rather than from cooperative hunting alone.

From an ecological perspective, the simulations suggest that ecosystems characterized by high predation efficiency, strong cooperation, and reduced handling time may exhibit oscillatory dynamics at relatively low population densities. In contrast, systems with moderate predation intensity and weaker cooperation can sustain higher predator densities with smoother convergence toward equilibrium. Moreover, prey immigration ($c = 1$) contributes to satisfying the analytical existence condition for a positive coexistence equilibrium under the considered parameter regimes.

3.3.4. Time-series dynamics for contrasting parameter regimes

Time-series simulations illustrate transient dynamics under two distinct parameter sets. Fig. 3 displays solutions for the **baseline parameter regime** with moderate predation efficiency ($\beta = 0.1$) and weak cooperative hunting ($\alpha = 0.05$). Fig. 4 shows the **high-efficiency regime**, which combines strong predation ($\beta = 3.1$) with heightened cooperation ($\alpha = 0.5$) and modified predator demographic parameters.

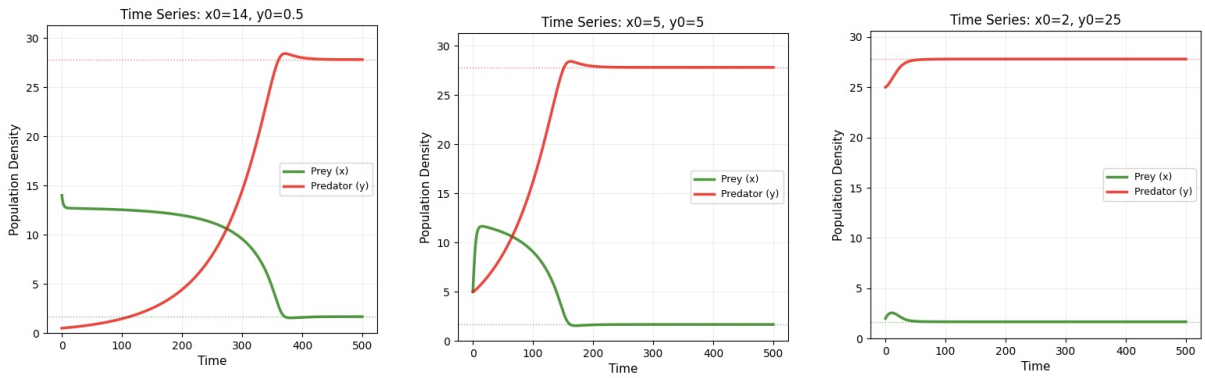

(a) $x(0) = 14$, $y(0) = 0.5$ (b) $x(0) = 5$, $y(0) = 5$ (c) $x(0) = 2$, $y(0) = 25$

Fig. 3: Time-series for the baseline parameter regime: $\beta = 0.1$, $\alpha = 0.05$, $m = 4$, $\mu = 0.04$, $d = 0.02$, $r = 0.28$, $K = 10$, $c = 1$. Green: prey; red: predator. All trajectories converge to the coexistence equilibrium $E_2 \approx (1.6735, 27.8033)$.

Baseline regime ($\beta = 0.1$). Three trajectories with different initial conditions (Fig. 3) all approach the predator-dominated equilibrium $E_2 \approx (1.6735, 27.8033)$. The prey (green curves) typically show an initial overshoot followed by gradual decay, while predators (red) grow steadily toward their equilibrium value. Convergence requires 300–500 time units, with mild transient

oscillations apparent in case (c). This slow, predominantly monotonic approach agrees with the stable-node classification derived from eigenvalue analysis ($\lambda_1 \approx -0.1670$, $\lambda_2 \approx -0.0562$, both real and negative).

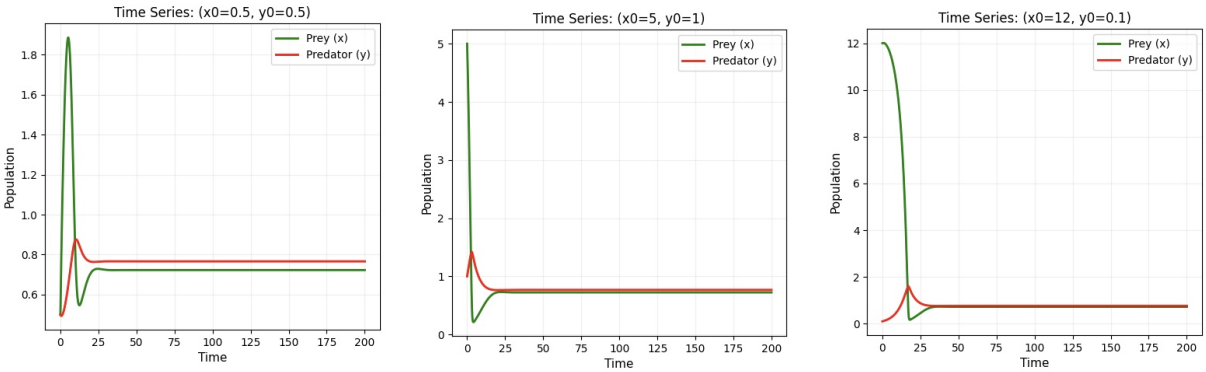

(a) $x(0) = 0.5$, $y(0) = 0.5$ (b) $x(0) = 5$, $y(0) = 1$ (c) $x(0) = 12$, $y(0) = 0.1$

Fig. 4: Time-series for the high-efficiency regime: $\beta = 3.1$, $\alpha = 0.5$, $m = 1$, $\mu = 0.4$, $d = 0.2$, $r = 0.28$, $K = 10$, $c = 1$. This regime combines elevated attack rate, strong cooperative hunting, reduced handling time, and altered predator physiology. Green: prey; red: predator. All solutions converge to $E_2 \approx (0.7230, 0.7663)$.

High-efficiency regime ($\beta = 3.1$). Under this parameter set (Fig. 4), trajectories converge more rapidly (within 120–150 time units) to the nearly balanced coexistence equilibrium $E_2 \approx (0.7230, 0.7663)$. Pronounced damped oscillations are visible in all three subfigures, with a period of approximately 50 time units. The predator peaks consistently lag 10–15 time units behind the prey peaks. This oscillatory decay matches the stable-spiral classification ($\lambda \approx -0.2771 \pm 0.3068i$, complex with negative real parts).

Comparison and ecological interpretation. The two regimes exhibit stark differences in both equilibrium structure and transient dynamics. The baseline regime supports a high predator density ($y^* \approx 27.8$) that heavily suppresses prey ($x^* \approx 1.7$), with slow, monotonic convergence. In contrast, the high efficiency regime yields nearly equal population sizes ($x^* \approx 0.72$, $y^* \approx 0.77$) and shows a faster, oscillatory approach to equilibrium.

Transition in stability type. The coexistence equilibrium exhibits different stability types in the two regimes: a stable node in the baseline case ($\alpha = 0.05$) and a stable spiral in the high-efficiency case ($\alpha = 0.5$). Although multiple parameters differ between these scenarios—including the attack rate β, cooperation intensity α, handling time m, and predator life history traits μ, d—the contrast illustrates the model's capacity to generate both monotonic and oscillatory convergence under biologically plausible parameter combinations.

Node-to-spiral threshold. The transition from stable node to stable spiral occurs when the discriminant $\Delta_s = T^2 - 4D$ of the characteristic polynomial changes sign. Holding all other parameters fixed at their baseline values, numerical evaluation of the Jacobian at the coexistence equilibrium shows that $\Delta_s = 0$ at an approximate critical value $\alpha_c \approx 0.24$. For $\alpha < \alpha_c$, the eigenvalues are real and negative (stable node), whereas for $\alpha > \alpha_c$ they form a complex conjugate pair with negative real part (stable spiral). This indicates that variation in cooperative hunting intensity alone is sufficient to induce the node-to-spiral transition when other parameters are fixed, although a full analytical bifurcation analysis is beyond the present scope.

Ecologically, the simulations suggest that ecosystems with efficient predators and strong cooperative hunting may exhibit tighter coupling and quicker recovery from perturbations, albeit

at lower overall population levels. Weaker predation combined with modest cooperation can sustain much larger predator populations, but with slower response times. In both regimes, constant prey immigration ($c = 1$) contributes to satisfying the analytical existence condition for a positive coexistence equilibrium.

4. Conclusion

This study investigated the dynamics of a predator–prey model integrating two key ecological mechanisms: constant prey immigration and cooperative hunting among predators. The primary objective was to analyze how these combined factors influence equilibrium structure, stability properties, and population coexistence.

The main findings demonstrate that the proposed model exhibits biologically meaningful equilibria whose stability depends critically on parameter values. Analytically, we established the existence of a predator-free equilibrium E_1 and established sufficient conditions for the existence and uniqueness of a coexistence equilibrium E_2, deriving explicit stability criteria through eigenvalue analysis of the Jacobian matrix. For the predator-free equilibrium $E_1 = (x_1, 0)$, we showed that x_1 increases with the immigration rate c, exceeding the carrying capacity K when $c > 0$. The coexistence equilibrium exists when $\mu > d$ and is characterized by an explicit algebraic relationship between prey density, predator density, and the cooperation parameter.

Numerical simulations with a baseline parameter set revealed a coexistence equilibrium E_2 that is a stable node (eigenvalues $\lambda_1 \approx -0.1670$, $\lambda_2 \approx -0.0562$), ensuring monotonic convergence near equilibrium. The predator-free equilibrium E_1 acts as a saddle point, unstable to predator invasion due to immigration-maintained prey availability.

Phase-portrait and time-series analyses highlighted how different parameter regimes affect system dynamics. Under a high-efficiency regime that combines elevated attack rate ($\beta = 3.1$) with strong cooperative hunting ($\alpha = 0.5$) and modified predator traits, the coexistence equilibrium becomes a stable spiral ($E_2 \approx (0.7230, 0.7663)$) exhibiting damped oscillatory convergence. In contrast, the baseline regime with moderate predation and weak cooperation yields a stable node with direct convergence. **This contrast illustrates a node-to-spiral transition** associated with increased cooperation intensity and predation efficiency. A sensitivity analysis varying α alone (with other parameters fixed) identified a critical threshold $\alpha_c \approx 0.24$, above which the stable node becomes a stable spiral, indicating that cooperative hunting intensity can independently induce this qualitative change when other parameters are held fixed. Although multiple parameters differ between the two regimes, the shift demonstrates the model's capacity to generate both monotonic and oscillatory convergence under biologically plausible conditions.

The integration of prey immigration and cooperative hunting offers important theoretical insights. Immigration reduces extinction risk for the prey population and enlarges the parameter region supporting coexistence while cooperative hunting modifies both equilibrium densities and transient dynamics. Weak cooperative hunting supports higher predator densities but stabilizes dynamics through direct convergence, whereas strong cooperation—especially when combined with efficient predation—can introduce oscillatory behavior, albeit at lower population levels.

These findings contribute to ecological theory by demonstrating how bottom-up (immigration) and top-down (cooperation) processes interact to shape predator–prey dynamics. The model provides a unified framework for analyzing systems where both mechanisms operate simultaneously, offering predictions testable against empirical data from natural or managed ecosystems.

Future directions. While this study establishes the basic dynamical properties of the integrated model, several extensions warrant investigation: (i) a systematic bifurcation analysis to analytically derive the exact parameter thresholds for the node-to-spiral transition (numerically estimated here as $\alpha_c \approx 0.24$); (ii) analytical investigation of global stability properties; (iii) stochastic and spatial extensions incorporating environmental variability and metapopulation

structure; and (iv) empirical validation using field data from systems with documented cooperative hunting and immigration patterns.

CRediT Authorship Contribution Statement

Naufal Daffa Faustin: Conceptualization, Methodology, Writing–Original Draft, Visualization, Writing–Review & Editing. **Dian Savitri:** Data Curation, Formal Analysis, Project Administration, Validation.

Declaration of Generative AI and AI-assisted technologies

No generative AI or AI-assisted technologies were used during the preparation of this manuscript.

Declaration of Competing Interest

The authors declare no competing interests.

Funding and Acknowledgments

This research received no external funding.

Data and Code Availability

Code analyzed during the current study are publicly available in the Google Colab [1].

References

[1] E. Gonzalez-Olivares, R. Lopez-Cruz, and A. Rojas-Palma, "Prey refuge use: Its impact on the dynamics of the lotka–volterra model," *Selecciones Matemáticas*, vol. 9, 2022. DOI: 10.17268/sel.mat.2022.02.06.

[2] A. H. Alridha, A. S. Al-Jilawi, and F. H. A. Alsharify, "Review of mathematical modelling techniques with applications in biosciences," *Iraqi Journal for Computer Science and Mathematics*, vol. 3, no. 15, pp. 135–144, 2022. DOI: 10.52866/ijcsm.2022.01.01.015.

[3] A. Hammoum, T. Sari, and K. Yadi, "The rosenzweig–macarthur graphical criterion for a predator–prey model with variable mortality rate," *Qualitative Theory of Dynamical Systems*, vol. 22, no. 1, p. 36, 2023. DOI: 10.1007/s12346-023-00739-6.

[4] A. Surendran, M. Plank, and M. Simpson, "Small-scale spatial structure affects predator-prey dynamics and coexistence," *Theoretical Ecology*, vol. 13, no. 4, pp. 537–550, 2020. DOI: 10.1007/S12080-020-00467-6.

[5] J. Alebraheem, T. Q. Ibrahim, G. E. Arif, A. A. Hamdi, O. Bazighifan, and A. H. Ali, "The stabilizing effect of small prey immigration on competitive predator-prey dynamics," *Mathematical and Computer Modelling of Dynamical Systems*, vol. 30, no. 1, pp. 605–625, 2024. DOI: 10.1080/13873954.2024.2366337.

[6] E. Diz-Pita and M. Victoria, "Predator–prey models: A review of some recent advances," *Mathematics*, vol. 9, no. 15, p. 1783, 2021. DOI: 10.3390/math9151783.

[7] S. Fu and H. Zhang, "Effect of hunting cooperation on the dynamic behavior for a diffusive holling type ii predator–prey model," *Communications in Nonlinear Science and Numerical Simulation*, vol. 99, p. 105 807, 2021. DOI: 10.1016/j.cnsns.2021.105807.

[1] https://colab.research.google.com/drive/1jA_-89T78_0kAwGm8HV3Y5W933l_IQFs?usp=sharing

[8] M. Chen and W. Yang, "Role of cooperative hunting among predators and predator–dependent prey refuge behavior in a predator–prey model," *Journal of Nonlinear Modeling and Analysis*, vol. 7, no. 2, pp. 209–226, 2025. DOI: 10.12150/jnma.2025.209.

[9] C. Peng and J. Jiang, "Dynamical regimes in a delayed predator–prey model with predator hunting cooperation: Bifurcations, stability, and complex dynamics," *Modelling*, vol. 6, no. 3, 2025. DOI: 10.3390/modelling6030084.

[10] I. Sendina-Nadal et al., "Diverse strategic identities induce dynamical states in evolutionary games," *Phys. Rev. Res*, vol. 2, p. 043 168, 2020. DOI: 10.1103/PhysRevResearch.2.043168.

[11] T. Borofsky, W. Marcus, and Y. Ram, "Cultural transmission, competition for prey, and the evolution of cooperative hunting," *Theoretical Population Biology*, vol. 156, pp. 12–21, 2024. DOI: 10.1016/j.tpb.2023.12.005.

[12] V. Groner et al., "Harmonizing nature's timescales in ecosystem models," *Trends in Ecology and Evolution*, vol. 40, no. 6, pp. 575–585, 2025. DOI: 10.1016/j.tree.2025.03.011.

[13] S. R. J. Jang and A. M. Yousef, "Effects of prey refuge and predator cooperation on a predator–prey system," *Journal of Biological Dynamics*, vol. 17, no. 1, 2023, Art. no. 2242372. DOI: 10.1080/17513758.2023.2242372.

[14] S. Samaddar, M. Dhar, and P. Bhattacharya, "Local stability analysis of a predator-prey dynamics incorporating both species density increasing functional response," *Journal of Mechanics of Continua and Mathematical Sciences*, vol. 17, no. 1, pp. 81–87, 2022. DOI: 10.26782/jmcms.2022.01.00006.

[15] C. Chen, X.-W. Wang, and Y.-Y. Liu, *Stability of ecological systems: A theoretical review*, 2024. DOI: 10.48550/arxiv.2312.07737.

[16] A. Das, S. Mandal, and S. K. Roy, "Prey-–predator model with allee effect incorporating prey refuge with hunting cooperation," *Journal of Biological Systems*, vol. 33, no. 02, pp. 519–552, 2025. DOI: 10.1142/S0218339025500135.

[17] J. Massing and T. Gross, "Generalized structural kinetic modeling: A survey and guide," *Frontiers in Molecular Biosciences*, vol. 09, no. 825052, p. 19, 2022. DOI: 10.3389/fmolb.2022.825052.

[18] X. Wang and A. Smit, "Studying the fear effect in a predator–prey system with apparent competition," *Discrete and Continuous Dynamical Systems - B*, vol. 28, no. 2, pp. 1393–1413, 2023. DOI: 10.3934/dcdsb.2022127.

[19] N. Min, H. Zhang, X. Gao, and P. Zeng, "Impacts of hunting cooperation and prey harvesting in a leslie-gower prey-predator system with strong allee effect," *AIMS Mathematics*, vol. 09, no. 12, pp. 34 618–34 646, 2024. DOI: 10.3934/math.20241649.

[20] S. Pal, F. Al Basir, and S. Ray, "Impact of cooperation and intra–specific competition of prey on the stability of prey–predator models with refuge," *Mathematical and Computational Applications*, vol. 28, no. 4, 2023. DOI: 10.3390/mca28040088.

[21] F. Kangalgil and S. Isık, "Effect of immigration in a predator–prey system: Stability, bifurcation and chaos," *AIMS Mathematics*, vol. 7, no. 8, pp. 14 354–14 375, 2022. DOI: 10.3934/math.2022791.

[22] A. P. Krishchenko and E. S. Tverskaya, "Analysis of systems with non-negative variables using the localization method," in *2020 15th International Conference on Stability and Oscillations of Nonlinear Control Systems (Pyatnitskiy's Conference) (STAB)*, 2020, pp. 1–4. DOI: 10.1109/STAB49150.2020.9140473.